

## MIT Open Access Articles

*Identification of illicit street drugs with swept#source Raman spectroscopy*

The MIT Faculty has made this article openly available. **Please share** how this access benefits you. Your story matters.

**Citation:** Kay, Kemberly XE, Atabaki, Amir H, Ng, Wei Bo, Li, Zheng, Singh, Gajendra P et al. 2022. "Identification of illicit street drugs with swept#source Raman spectroscopy." Journal of Raman Spectroscopy.

**As Published:** 10.1002/jrs.6357

**Publisher:** Wiley

**Persistent URL:** <https://hdl.handle.net/1721.1/143848>

**Version:** Final published version: final published article, as it appeared in a journal, conference proceedings, or other formally published context

**Terms of use:** Creative Commons Attribution NonCommercial License 4.0



# Identification of illicit street drugs with swept-source Raman spectroscopy

Kemberly X. E. Kay<sup>1,2</sup> | Amir H. Atabaki<sup>3</sup>  | Wei Bo Ng<sup>1</sup> | Zheng Li<sup>3</sup> |  
Gajendra P. Singh<sup>2</sup> | Stella W. L. Tan<sup>1,2</sup> | Rajeev J. Ram<sup>2,3</sup>

<sup>1</sup>Forensic Science Research Laboratory,  
Department of Biological Sciences,  
Faculty of Science, National University of  
Singapore, Singapore

<sup>2</sup>Disruptive & Sustainable Technologies  
for Agricultural Precision, Singapore-MIT  
Alliance for Research and Technology,  
Singapore

<sup>3</sup>Massachusetts Institute of Technology,  
CambridgeMassachusetts, USA

## Correspondence

Amir H. Atabaki, Massachusetts Institute  
of Technology, Cambridge, MA USA.  
Email: [atabaki@mit.edu](mailto:atabaki@mit.edu)

## Funding information

National Research Foundation Singapore

## Abstract

The identification of the illicit substances in low-purity seized drugs with Raman spectroscopy is an outstanding problem. The low concentration of the target molecule demands high sensitivity and the presence of impurities produces a strong fluorescence background that makes identification challenging. Although Raman analyzers with 785 and 830 nm excitation wavelengths provide high sensitivity, the longer 1064 nm wavelength produces lower fluorescence. In this work, we demonstrate a Raman spectrometer that simultaneously achieves both high sensitivity and low background fluorescence. We utilize swept-source Raman spectroscopy in which the spectrometer is replaced by a single high-collection spectral channel, and the Raman spectrum is swept using a tunable laser. By eliminating the spectrometer and its slit, the optical throughput and sensitivity are improved. Moreover, our swept-source system requires a single uncooled silicon photodiode that provides higher quantum efficiency at longer wavelengths compared with CCDs. This allowed us to use excitation wavelengths in the 900 nm range to reduce background fluorescence without sacrificing sensitivity. We have demonstrated 6x background fluorescence reduction in colored seized drugs compared with 830 nm excitation. With lower background fluorescence and high sensitivity, we could identify heroin with only 1% purity in a seized sample. Besides forensics and security, the demonstrated swept-source Raman spectroscopy approach can be a powerful technique in biomedical applications where strong background fluorescence limits detection capabilities.

## KEYWORDS

illicit drug, swept source

## 1 | INTRODUCTION

Kemberly X. E. Kay and Amir H. Atabaki contributed equally to this work.

Drug abuse is a prevalent and growing issue that affects all regions of the world. Between 2009 and 2018, global

This is an open access article under the terms of the [Creative Commons Attribution-NonCommercial](https://creativecommons.org/licenses/by-nc/4.0/) License, which permits use, distribution and reproduction in any medium, provided the original work is properly cited and is not used for commercial purposes.

© 2022 The Authors. *Journal of Raman Spectroscopy* published by John Wiley & Sons Ltd.

drug users had increased by 28%.<sup>[1]</sup> In 2018 alone, it was estimated that one in every 19 people in the world had used drugs at least once in the previous year.<sup>[1]</sup> Globally, cannabis, opioids, methamphetamine, ecstasy and cocaine remain the most abused drugs<sup>[1]</sup> and have been linked to high rates of fatal drug overdoses. In the United States, 70,200 drug overdose deaths in 2017 represented a 84.7% increase from 2010,<sup>[2]</sup> and two-thirds of these deaths were attributed to opioids.<sup>[1]</sup>

Besides being a public health threat, drug abuse imposes substantial economic burden. In Singapore, the annual economic impact of drug crimes amounts to approximately two billion dollars and 95% of the cost is accounted by heroin and methamphetamine.<sup>[3]</sup>

There are many reports<sup>[4–9]</sup> that purity levels of illicit street drugs vary significantly as they either contain impurities resulting from the manufacturing process or adulterated with cutting agents. The deadliest drugs are typically the potent compounds that come in small concentrations, such as heroin and fentanyl (Table 1). Heroin, one of the most common opioids, is often adulterated regardless of its geographical origin.<sup>[10]</sup> In the United States, the street forms are frequently mixed with fentanyl,<sup>[11]</sup> whereas Southeast Asian Heroin (Heroin No. 3) are heavily diluted with caffeine.<sup>[12]</sup> Furthermore, drug purities can vary widely in different regions of the country (shown in Table 1) and its unpredictable composition can increase the risks of overdose deaths. Therefore, the detection of low-purity drugs should have the highest priority for battling the harms of illicit substances.

Raman spectroscopy is an effective tool for the law enforcement, border police and first responders to analyze substances that could endanger the public in the field.<sup>[13]</sup> The screening process with Raman analyzers is quick, works through most packaging materials, and does not require contact with the sample. This is important as many potent illicit drugs such as fentanyl can be harmful if they come into contact with skin. Despite these ideal features for “field” analysis and screening, portable and handheld Raman analyzers have their limitations.

Most portable and handheld Raman analyzers do not provide sufficient sensitivity for the detection of low-purity, potent drugs. This is largely due to two factors: (1) sensitivity-size tradeoff of dispersive spectrometers and (2) the shot noise from the strong fluorescence emission from “cutting agents.” Most portable Raman analyzers today utilize dispersive spectrometers that have an inherent tradeoff between size, spectral resolution, and optical throughput that determines the sensitivity.<sup>[14]</sup> As a result, portable Raman analyzers cannot match the sensitivity level of laboratory-scale analyzers that provide the

sensitivity levels needed for the detection of illicit substances.

The second issue with low-purity illicit substances is the fluorescence emission from impurities and cutting agents. The shot noise from the fluorescence can limit the sensitivity and potential for detecting illicit substances. In particular, strong fluorescence emission with Raman analyzers that use 785 nm and 830 nm excitation wavelengths have been reported in the analysis of illicit drugs.<sup>[15–18]</sup> Fluorescence emission weakens as the excitation wavelength is increased, and therefore, Raman analyzers with 1064 nm excitation wavelength have been developed to reduce fluorescence background. These analyzers are shown to produce higher quality Raman spectra for many illicit substances including colored pills.<sup>[18,19]</sup> Nevertheless, these analyzers need InGaAs infrared detector arrays which are significantly noisier than their silicon counterparts, such as charged coupled devices (CCDs) used in 785 nm and 830 nm analyzers. This leads to low detection sensitivity, and therefore, although 1064 nm analyzers are effective for reducing fluorescence emission, they do not provide adequate sensitivity for the detection of low-purity drugs.

An alternative approach that has worked successfully for the detection of low-purity fentanyl and heroin is surface-enhanced Raman spectroscopy (SERS).<sup>[20]</sup> However, SERS requires dissolving the illicit substance in a solution and, therefore, does not preserve some of the benefits of spontaneous Raman spectroscopy such as being non-contact or non-invasive. This is important in cases where exposure of the illicit substance could be dangerous to law enforcement, or when the amount of seized illicit substance is too small for multiple experiments that involve wet chemistry and reagents. In the forensic context, evidence destruction disallows the re-examination of such trace evidence in the event that post-conviction testing is required. Non-invasive, reagent-less detection of low-purity drugs still remains an outstanding problem.

In this work, we have developed a Raman analyzer to provide both high sensitivity and low background fluorescence. This is mainly achieved by moving the excitation wavelength to the 900 nm range and using low-noise silicon detectors with high quantum efficiency in the near-infrared range. The 900 nm excitation wavelength reduces fluorescence compared with 785 and 830 nm analyzers, whereas the silicon detector provides low noise for achieving high sensitivity. In order to maximize the excitation wavelength and reduce fluorescence, we utilize swept-source Raman spectroscopy.<sup>[21]</sup> This approach allows us to eliminate the dispersive spectrometer and the wavelength limitations imposed by the low quantum efficiency of CCDs at longer wavelengths. We use a large-

TABLE 1 Purity levels of the most abused drugs in the world

Drug	Purity	Common cutting agents <sup>[22]</sup>	Previous Raman work on 785 nm systems	
Heroin	67% (27%–77%) Vietnam, 2017 <sup>[9]</sup>	Caffeine, Chloroquine, Dextromethorphan, Paracetamol, Piracetam, Procaine, Quinine, Sugars, Theophylline	Detectable down to 60% w/w heroin in quinine <sup>[24]</sup>	
	63%–73% Cambodia, 2017 <sup>[9]</sup>			
	50% US, 2018 <sup>[23]</sup>			Undetectable with strong background fluorescence <sup>[18]</sup>
	16%–59% Australia, 2015–2018 <sup>[4,5]</sup> 9%–57% Europe, 2010–2017 <sup>[7,8]</sup> 3% (1%–5%) Singapore, 2018 <sup>[9,12]</sup>			Some Raman peaks detectable down to ~25% w/w heroin <sup>[25]</sup>
Fentanyl	9.7% (0.05%–98%) US, 2019 <sup>[6]</sup>	Heroin, Cocaine		
Methamphetamine (crystalline)	95% Thailand, 2019 <sup>[1]</sup>	Ammonium acetate, Caffeine, Dimethylsulfone, MSM	Detectable down to 30% w/w methamphetamine in dimethylsulfone <sup>[24]</sup>	
	78% Indonesia, 2017 <sup>[9]</sup>			
	75% (40%–80%) Malaysia, 2018 <sup>[9]</sup>			
	70% (42%–75%) Vietnam, 2017 <sup>[9]</sup>			
	68%–78% Cambodia, 2017 <sup>[9]</sup>			
	49%–83% Australia, 2015–2018 <sup>[4,5]</sup> 5%–90% Europe, 2010–2017 <sup>[7,8]</sup>			
Amphetamine	5%–50% Europe, 2010–2017 <sup>[7,8]</sup>	Caffeine, Ephedrine, Paracetamol	Detectable with background fluorescence <sup>[18]</sup>	
	1%–77% Australia, 2015–2018 <sup>[4,5]</sup>			
MDMA	39% Philippines, 2016 <sup>[9]</sup>	Amphetamine, Caffeine, Chloroquine, Dextromethorphan, Ketamine, Methamphetamine, NPS, Paracetamol, PMA, PMMA	Almost undetectable due to background fluorescence <sup>[18]</sup>	
	36% Singapore, 2015 <sup>[26]</sup>			
	30% (19%–43%) Vietnam, 2017 <sup>[9]</sup> 29%–39% Cambodia, 2017 <sup>[9]</sup>			Some Raman peaks detectable down to 10% w/w MDMA <sup>[25]</sup>
	15%–40% Malaysia, 2018 <sup>[9]</sup>			
Cocaine	73%–83% Cambodia, 2017 <sup>[9]</sup>	Caffeine, Diltiazem, Hydroxyzine, Levamisole, Lidocaine, Phenacetin, Procaine, Starch, Talc, Tetramisole	Crack cocaine was undetectable due to background fluorescence <sup>[18]</sup>	
	65% US, 2018 <sup>[27]</sup>			
	32%–62% Australia, 2015–2018 <sup>[4,5]</sup>			Some Raman peaks detectable down to 10% w/w cocaine HCl <sup>[25]</sup>
	10%–88% Europe, 2010–2017 <sup>[7,8]</sup>			
Ketamine	75% (70%–85%) Malaysia, 2018 <sup>[9]</sup>	Caffeine, Dimethylsulfone, Diphenhydramine, Lidocaine, Procaine		
	59% (12%–84%) Vietnam, 2017 <sup>[9]</sup>			
	49%–59% Cambodia, 2017 <sup>[9]</sup>			

area amplified silicon photodiode that provides double-digit quantum efficiency at wavelengths as high as 1100 nm, beyond what is achievable even in the advanced deep-depletion CCDs. The elimination of the spectrometer also allows improving the throughput and the overall sensitivity of the analyzer. This is critical for the detection of low-purity drugs.

**TABLE 2** Specifications of the commercial micro-Raman and in-house SSRS analyzers

Parameter	Micro-Raman analyzer	Swept-source Raman analyzer
Excitation wavelength	830 nm	925–980 nm
Laser power	58 mW	10 mW
Spectral range	200–2700 cm <sup>-1</sup>	450–1350 cm <sup>-1</sup>
Spectral resolution	8 cm <sup>-1</sup>	5 cm <sup>-1</sup>
Numerical aperture of objective	0.13	0.63
Detector	TE-cooled back-illuminated CCD (2048 pixel)	Amplified silicon photodiode

**TABLE 3** List of illicit street drugs studied

Category	Identifier	Drug	Color	Purity (%)	% HQI Dispersive	% HQI SSRS
White or colorless	S1	Methamphetamine	White	66	97 ± 0.03	96 ± 0.21
	S2	Methamphetamine	White	66	96 ± 0.30	96 ± 0.72
	S3	Methamphetamine	White	64	97 ± 0.4	95 ± 0.4
	S4	Methamphetamine	White	67	97 ± 0.31	97 ± 0.04
	S5	Ketamine	White	71	96 ± 0.14	92 ± 1.0
	S6	Ketamine	White	73	97 ± 0.29	93 ± 1.0
	S7	Ketamine	White	67	95 ± 0.81	90 ± 5.3
	S8	Cocaine	White	54	93 ± 0.19	96 ± 0.03
	S9	Gamma-butyrolactone	Colorless	NR	98 ± 0.03	96 ± 0.22
Colored	S10	Methamphetamine	Brown	NR	59.7	64.3
	S11	Heroin No. 3	Brown	1	NA	NA
	S12	MDMA	Pink	38	73.5	70.5
	S13	MMB-FUBINACA, N-ethylpentylone	Blue	NR	9.3	19.05

*Note:* The 1% concentration of the heroin sample is too low to use a traditional HQI definition for identifying the target chemical. In Section 3.4 we employ a different method for identifying Raman peaks of low-purity samples.

Abbreviation: NR, not reported.

## 2 | MATERIALS AND METHODS

### 2.1 | Illicit street drug samples

We analyzed 13 seized street samples that were provided by the Central Narcotics Bureau in Singapore as listed in Table 2. The identities of the drugs and their purities were previously confirmed with gas chromatography-mass spectrometry (GC-MS) by the Health Sciences Authority in Singapore. All samples were in powder form and sealed in transparent polyethylene bags, except for liquid gamma-butyrolactone contained in a sealed bottle. Powder samples were analyzed through the transparent bags whereas an aliquot of gamma-butyrolactone was transferred to a quartz cuvette for Raman measurements.

### 2.2 | Overview of Raman analyzers

We used two back-scattered Raman spectroscopy systems for our experiments: (1) a dispersive micro-Raman analyzer with 830 nm excitation wavelength (Technospex, uRaman-Ci) and (2) our in-house swept-source Raman spectroscopy (SSRS) system with excitation wavelengths from 925 to 980 nm. This allowed us to compare the SSRS system with 830 nm Raman analyzers that have gained interest for forensics and security applications.<sup>[28]</sup> Table 3

compares the main specifications of these spectroscopy systems.

We had several criteria for the design of the SSRS system: (1) a high spectral resolution on the order of  $5\text{ cm}^{-1}$  for resolving the sharp Raman peaks of illicit substances in solid form; (2) a spectral range coverage of  $500\text{--}1200\text{ cm}^{-1}$  overlapping with the main Raman peaks of the illicit substances in our study; (3) the longest excitation wavelength possible with low-noise near-infrared silicon detectors; (4) a high-throughput optical design to achieve the sensitivity needed for low-purity drugs. The SSRS architecture requires a single spectral channel which could be optimized for both high optical throughput and long excitation wavelength. The SSRS architecture requires a single spectral channel which could be optimized for both high optical throughput and long excitation wavelength. The elimination of the spectrometer and its slit in this architecture improves the optical throughput. Also, the excitation wavelength could be increased beyond  $830\text{ nm}$  because of the availability of efficient single-element silicon photodiodes above  $1000\text{ nm}$  wavelength. Below, we describe the concept of SSRS and the details of our instrument.

### 2.3 | Swept-source Raman spectroscopy

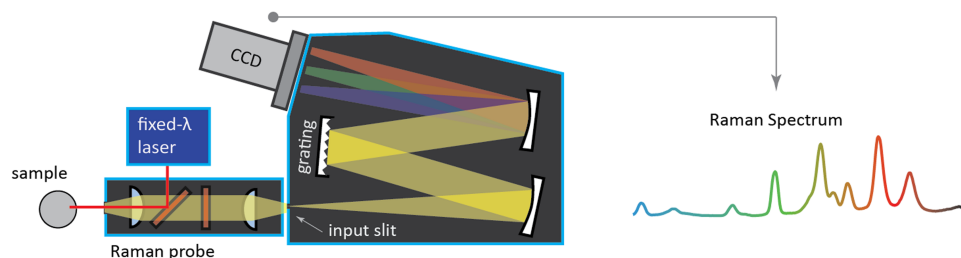
The swept-source Raman spectroscopy concept and instrument schematic are shown in Figure 1 and compared with dispersive Raman spectroscopy. In the SSRS approach, the spectrometer is replaced by a single high-throughput spectral channel and a tunable laser is used to sweep the Raman spectra through this one channel

(see Figure 1b). By removing the spectrometer and its micron-sized slit the optical throughput of the system can be increased. We use an ultra-narrowband, high-throughput Fabry–Perot interference filter and a millimeter-sized detector for implementing the single detection channel. The throughput (or etendue) of the SSRS setup developed in this work at every spectral channel is  $50\times$  higher than the dispersive spectrometer in the micro-Raman system. This throughput advantage has allowed us to both lower the laser power by almost  $6\times$  ( $10\text{ mW}$ ) and use lower cost uncooled detectors instead of cooled CCDs. The laser power in the SSRS setup is only twice the ANSI Z136.1 standard for ocular exposure.

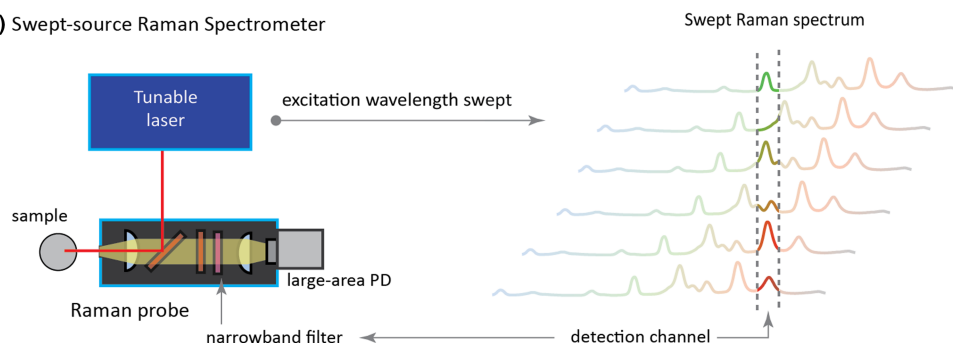
The schematic of the experimental SSRS setup is shown in Figure 2a. We use a benchtop fiber-coupled external-cavity laser (Sacher GmbH, Germany) with a tuning range of  $920\text{--}985\text{ nm}$ , an output power of  $15\text{ mW}$  for excitation and a linewidth of  $1\text{ MHz}$ . The excitation laser is collimated, passed through amplified spontaneous emission filters, and delivered to the optical assembly (marked Raman probe in Figure 2) that is used for excitation, as well as, collection and detection of the back-scattered Raman emission. The Raman emission is filtered through several thin film filters (including a ultra-narrow bandpass filter) and then focused on to an amplified single-channel silicon photodetector. We use an ultra-narrow bandpass filter (Alluxa Inc, USA) with a center wavelength of  $1031\text{ nm}$  and a full-width half maximum (FWHM) bandwidth of  $0.5\text{ nm}$ . This filter provides about  $5\text{ cm}^{-1}$  spectral resolution, and together with our

**FIGURE 1** (a) Dispersive Raman spectrometer with fixed excitation wavelength. A large benchtop dispersive spectrometer is needed to achieve high optical throughput due to the presence of the entrance slit. (b) Swept-source Raman spectroscopy concept in which a tunable excitation laser sweeps the Raman spectrum across a narrowband detection channel. The optical throughput of this architecture can be up to three orders of magnitude higher than the dispersive Raman spectrometer due to the elimination of the spectrometer slit [Colour figure can be viewed at [wileyonlinelibrary.com](http://wileyonlinelibrary.com)]

(a) Dispersive Raman Spectrometer



(b) Swept-source Raman Spectrometer



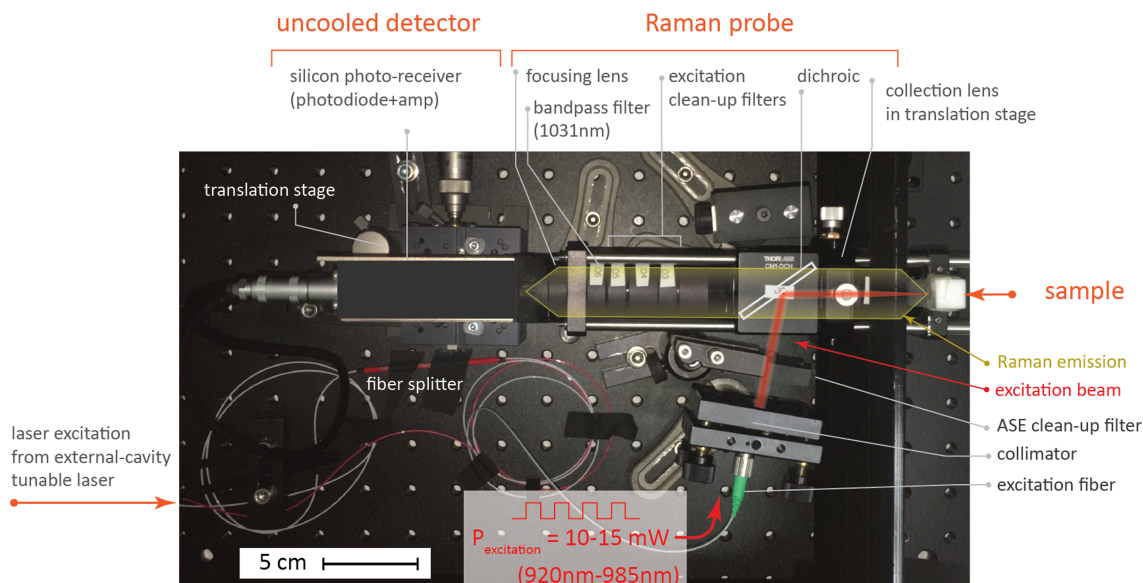


**FIGURE 2** The photo of SSRS setup with a back-scattered geometry. Excitation laser is delivered to the setup from an external-cavity semiconductor tunable laser with an optical fiber. The excitation laser is focused on the sample after passing through a 99:1 fiber splitter, a fiber collimator, two ASE cleanup filters and reflection off of a dichroic filter. The same lens is used for both excitation and collection of Raman emission. The collected light is passed through excitation cleanup filters and a narrowband filter with a 0.5 nm linewidth. The filtered Raman light is focused on to a 1.2 mm<sup>2</sup> silicon photodiode amplified with a high-gain transimpedance amplifier. The output of the detector is acquired on a computer with a data acquisition card [Colour figure can be viewed at [wileyonlinelibrary.com](http://wileyonlinelibrary.com)]

tunable laser cover a spectral range of 500–1300 cm<sup>-1</sup>. The detector in our experiment is an amplified uncooled silicon photodiode with an area of 1.21 mm<sup>2</sup> and sub-femtowatt sensitivity (Femto GmbH, Germany). See supporting information for further details of the setup.

## 2.4 | Spectral processing

The Raman spectra acquired from the dispersive Raman were truncated to 200–1750 cm<sup>-1</sup>, followed by cosmic ray removal by median filtering and smoothed with Savitzky-Golay filter. Raman data acquired from SSRS were truncated to 510–1250 cm<sup>-1</sup>. Polynomial fitting with non-negative constraint (lieberfit) was used to remove background in the Raman spectra acquired from both systems. Although the shape of background is different between the two systems, they could both be fit with a fifth-order polynomial. We also observed etaloning in the spectra with the dispersive system. We included an etaloning term in background fitting so its effect could be removed after background subtraction. See supporting information for more details.

For chemical verification, Raman spectra were uploaded to KnowItAll<sup>®</sup> spectral library (Wiley, USA) and a percentage hit quality index (HQI) correlation of several potential chemical identities was reported. The etaloning (oscillation behavior) observed in the spectra of

the dispersive system was removed prior to spectral library comparison.

## 3 | RESULTS AND DISCUSSIONS

### 3.1 | Chemical database and identification

The identity of each drug sample was evaluated by a correlation algorithm in KnowItAll<sup>®</sup> spectral library that contains the largest collection of Raman spectra of various drug reference standards measured predominantly with 1064 nm laser wavelength. The database adopted HQI as an indicator in spectral library matching for the identification of unknown materials. The measured spectrum of the unknown compound is correlated to all spectra of known compounds in the reference database, and the degree of similarity between the sample spectrum and each library spectrum is quantified by the calculation of HQI.

The KnowItAll<sup>®</sup> spectral library was able to identify the uncolored illicit substances but not the colored drugs. These colored substances have a significantly lower concentration of the illicit compound and higher impurities compared with uncolored drugs. The Raman peaks of the impurities mask the weak Raman peaks of the active compound and do not allow the KnowItAll<sup>®</sup> algorithm to robustly identify the active compound in colored drugs.

In Section 3.4, we use an optimization algorithm to find the contribution of the Raman spectrum of a target molecule present in low concentration to the Raman spectrum of colored drug samples.

### 3.2 | Uncolored illicit substances

All of the nine uncolored drug samples were successfully identified with the KnowItAll<sup>®</sup> spectral library for both the dispersive and swept-source Raman systems. These

are white powders with purity of >50% which include methamphetamine (S1–S4), ketamine (S5–S7), and cocaine (S8), as well as colorless liquid gamma-butyrolactone (GBL) (S9). Figure 3a shows the barchart of HQI of selected drug samples analyzed on both Raman systems which consistently reported high percentage hit of their respective drug identity above 90%. Figure 3b shows the Raman spectrum of four of the uncolored drugs acquired with both dispersive (orange) and swept-source (blue) Raman setups. The Raman spectra from these two approaches are in agreement. For the swept-

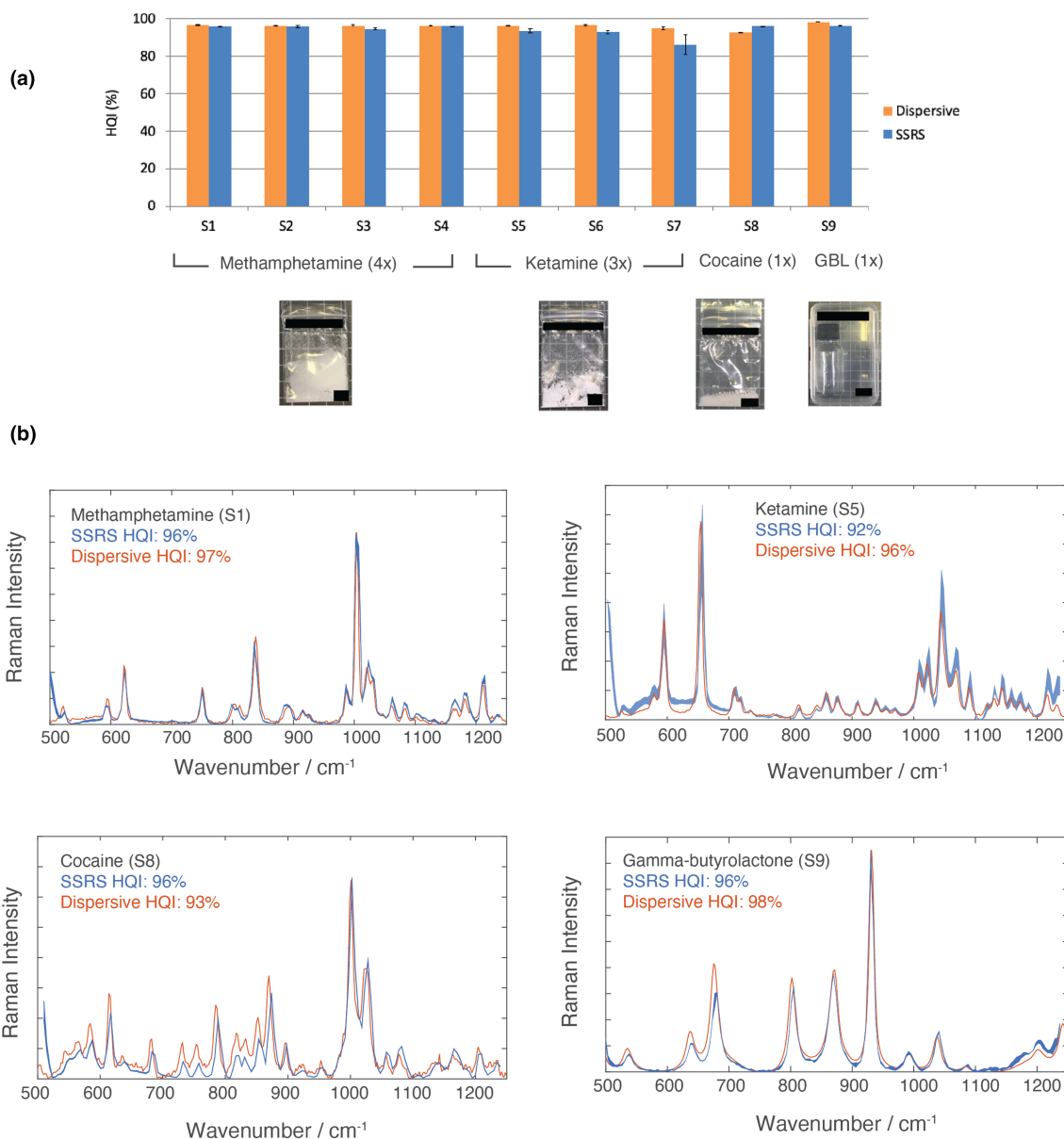


**FIGURE 3** Identification of illicit white powders and a colorless liquid. (a) Barchart comparing HQI of the spectra obtained from the dispersive and swept-source Raman systems for samples S1–S9 from Table 3. Four independent samples of methamphetamine, three independent samples of ketamine were measured. (b) The Raman spectrum of one sample from each drug type is shown for both the dispersive (orange) and swept-source (blue) Raman systems. Three swept-source Raman spectra were acquired and the variations between these measurements are shown by the shaded areas [Colour figure can be viewed at [wileyonlinelibrary.com](https://onlinelibrary.wiley.com)]

source measurements, three spectra were acquired and the shaped region in Figure 3b shows the variations between these measurements. The acquisition time with the dispersive micro-Raman system is 5, 4, 4, and 7 s for methamphetamine, ketamine, GBL and cocaine, respectively. The integration time is 1 s per spectral point for all drugs with the SSRS setup, resulting in 120 s of total acquisition time.

The similar HQI with both Raman systems validates that SSRS can be reliably used for identification of illicit substances even with spectra databases acquired with dispersive Raman analyzers. Some of the differences in the HQI in the two systems is because of the wavelength-dependent components that affect the spectra differently in these systems — for example, wavelength dependence of the detectors and filters. We expect HQI differences can be reduced through power transmission/reflection calibration.

Also, there are small differences between the Raman peak positions in the dispersive and swept-source systems seen in Figure 3b. We used a calibrated spectrometer to find a lookup table for wavelength tuning in the swept laser. However, in the Raman measurements there were slight deviations between the actual output wavelength and the wavelength in the lookup table. This has resulted in slight differences between the swept-source and dispersive spectra. In the future, we will use a miniature spectrometer to measure the wavelength in real-time for dynamic wavelength calibration.

### 3.3 | Colored illicit substances

Four of the seized drugs were colored, including brown substances (Heroin No. 3 and methamphetamine), pink MDMA and blue NPS. The color in Heroin No. 3 and methamphetamine is a result of impurities from the drug manufacturing process. Heroin is a semi-synthetic opioid that involves the initial collection of raw opium from opium poppy plant and subsequent chemical conversion to morphine, and finally, heroin. The brown coloration most likely originates from the opium gum and remains in the final heroin product due to poor purification which removes highly-colored opium alkaloid impurities.<sup>[29]</sup> Furthermore, because Heroin No. 3 is produced in the first stage of purification, it would contain lower concentration of diamorphine. Similarly, residual impurities may be retained in the final drug product synthesized from a different synthetic route or by a less-competent methamphetamine cooker,<sup>[30]</sup> as was the case with an unusual methamphetamine sample (S10) that appeared brown as opposed to its usual white color. On the other hand, different colored dyes can be intentionally added to

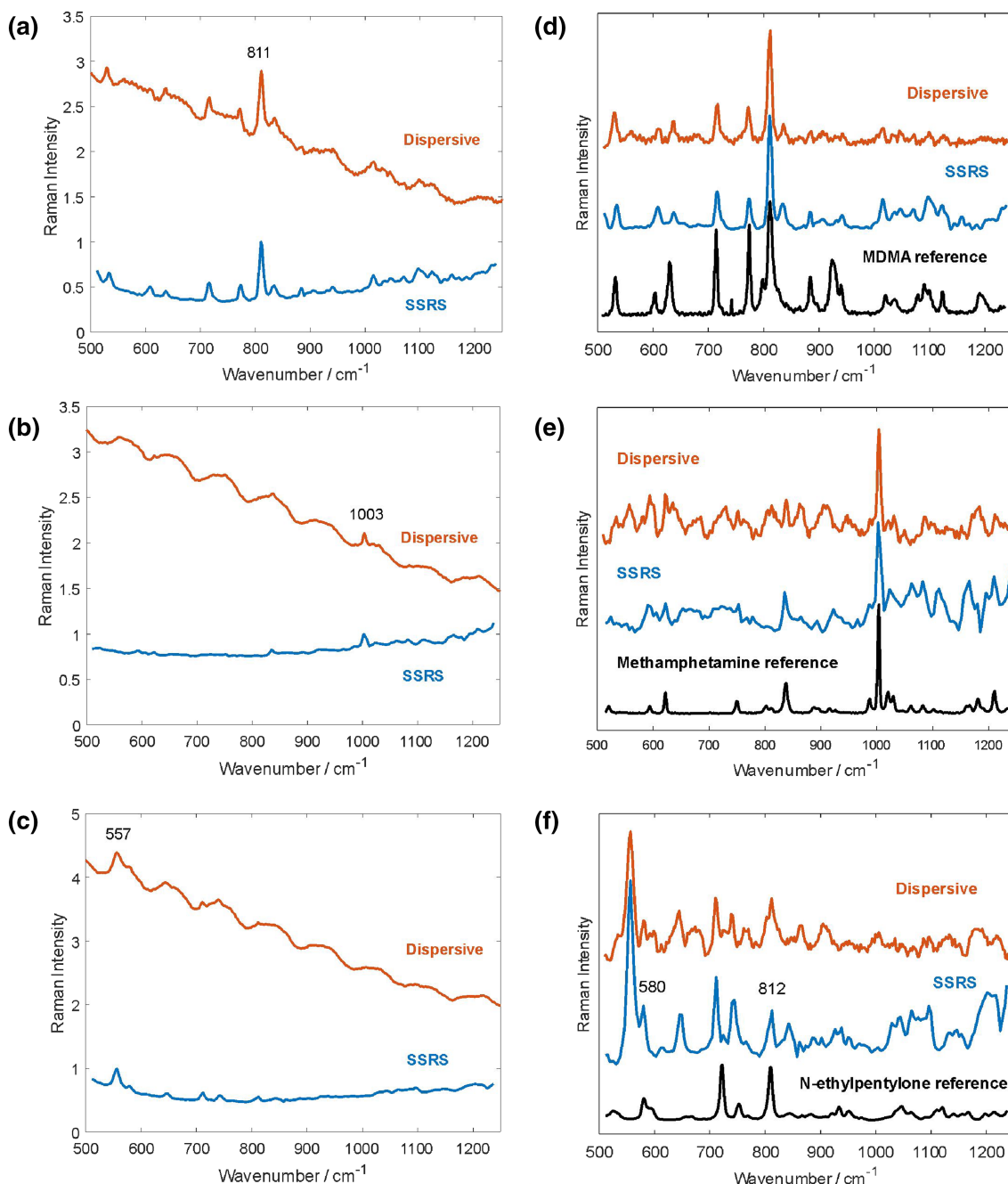
drugs not only to give them an eye-catching and attractive appearance, but also as a means of indicating the homogeneity of the adulterated mixture. This applies to ecstasy powders or tablets containing MDMA, and NPS that are passed off as ecstasy for their stronger stimulating effects.<sup>[31]</sup>

Figure 4 shows the Raman spectra of three of these colored drugs: methamphetamine (S10), MDMA (S12) and NPS (S13). Figures 4a–c and 4d–f show the spectra before and after background subtraction. The acquisition time is 5 and 120 s for the dispersive and SSRS systems, respectively. The background fluorescence in these drugs were significantly higher compared with uncolored drugs. This is caused by the impurities including the colored dye. Raman spectra in each of Figure 4a–c are normalized such that the strongest Raman peak of each sample has a similar height in both dispersive and swept-source systems. With this normalization, the relative background level in each figure represents the relative fluorescence signal in each system.

The background fluorescence in the SSRS setup is 2–5× lower compared with the dispersive Raman system due to its longer excitation wavelength. The difference in fluorescence emission between these systems is the strongest toward shorter wavenumbers. This is because the excitation wavelength in the SSRS setup increases toward shorter wavenumbers, and therefore, induces a weaker background fluorescence. SSRS also exhibits a much flatter fluorescence background compared with dispersive Raman spectroscopy: as the excitation wavelength increases, the fluorescence emission decreases whereas the offset between excitation and detection wavelengths decreases. These two effects move the fluorescence signal in opposite directions and lead to a notably flatter fluorescence background.

Figure 4d–f shows the Raman spectra of the same substances after background subtraction and removing etaloning (oscillating behavior) in the spectra of the dispersive spectrometer — see supporting information for etaloning removal. The Raman spectrum of the pure form of each illicit substance is also shown.

The KnowItAll<sup>®</sup> database failed to find the right chemical match for impure colored samples. This could be due to (1) the noisier spectra of these samples due to the lower concentration of active compounds and (2) the presence of impurities that are not in the database. Because the active compounds of these samples were determined with GC-MS, we estimated HQI by calculating the correlation coefficient between the Raman spectra of the sample and their main compound.<sup>[32]</sup> These HQI values are shown in Table 2. The HQI value drops with the purity of the sample as the correlation between the spectra of the sample and main compound is decreased.



**FIGURE 4** Raman spectra of colored drugs on both Raman systems. (a) MDMA (S12) showing its strongest peak at  $811\text{ cm}^{-1}$ , (b) brown methamphetamine (S10) with characteristic peak at  $1003\text{ cm}^{-1}$ , (c) NPS mixture (S13) normalized to most prominent Raman peak at  $557\text{ cm}^{-1}$ . Comparison of Raman spectra acquired from dispersive and swept-source systems to (d) MDMA, (e) methamphetamine, (f) *N*-ethylpentylone reference from KnowItAll<sup>®</sup> spectral library [Colour figure can be viewed at [wileyonlinelibrary.com](http://wileyonlinelibrary.com)]

This makes HQI less useful as a value that indicates the presence of a target compound in low-purity samples. As a result, we could not apply HQI to the heroin sample (S11) that only has a 1% purity level. In Section 3.4, we apply a Bayesian estimation algorithm for identifying target chemicals in low-purity samples.

### 3.4 | Low-purity heroin sample

Figure 5a shows the Raman spectra of a seized Heroin No. 3 sample (S11) with the swept-source and dispersive Raman systems. The purity level of heroin was estimated at 1% using mass spectrometry at Health Sciences

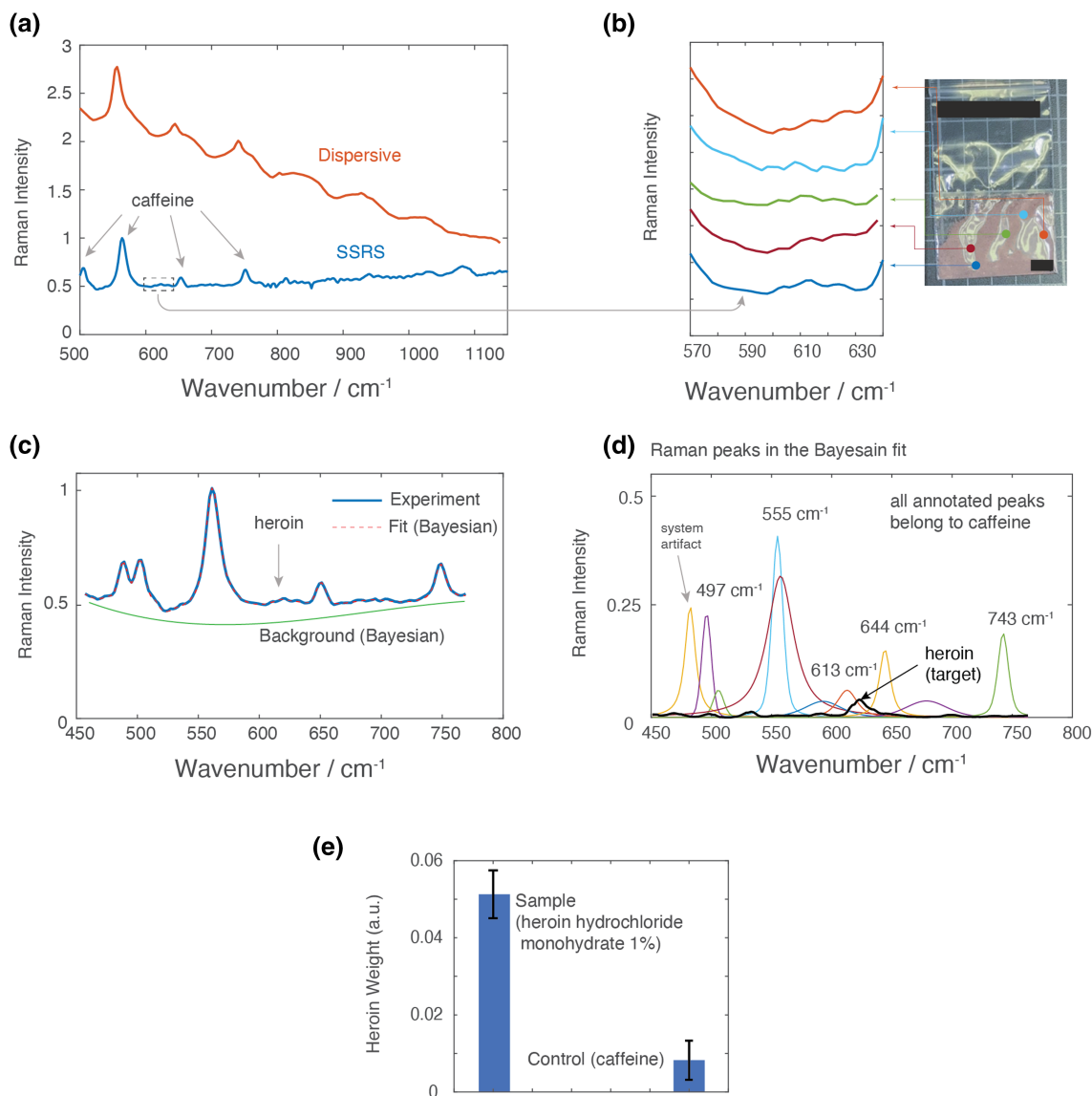


**FIGURE 5** (a) Raman spectra of the seized Heroin No. 3 sample with SSRS and dispersive Raman spectroscopy systems. (b) Swept-source Raman spectra from five different points on the seized sample near the strongest Raman peak of heroin around  $630\text{ cm}^{-1}$ . The bottom spectrum is the same spectrum shown in panel (a). (c) The result of the Bayesian fitting algorithm (dashed red) shown along with the experimental result (blue). The background that is modeled with spline functions in the Bayesian algorithm is shown in green. (d) Individual Raman peaks contributing to final fitting result. The contribution of heroin is also shown by the black curve. (e) The weight of the target molecule (heroin HCl monohydrate) estimated by the Bayesian algorithm for the seized sample and control (pure caffeine) [Colour figure can be viewed at [wileyonlinelibrary.com](http://wileyonlinelibrary.com)]

Authority (HSA), Singapore. Considering that the Raman scattering cross-section of heroin is known to be weak with only one major peak near  $625\text{ cm}^{-1}$ ,<sup>[33]</sup> the reduction of background fluorescence and its shot noise is important for identifying heroin in these low-purity samples. The longer excitation wavelength of the SSRS setup (925–980 nm) compared with the dispersive micro-Raman system (830 nm) helps in this regard by reducing the background fluorescence by about 4x as shown Figure 5a.

Four of the strongest Raman peaks observed in the spectra ( $497$ ,  $555$ ,  $644$ , and  $743\text{ cm}^{-1}$ ) are attributed to

caffeine which is a common cutting agent for illicit drugs (marked on Figure 5a). KnowItAll<sup>®</sup> spectral library also found a match to caffeine for this sample with an HQI of 94.6%. The strongest Raman peak of heroin at  $625\text{ cm}^{-1}$  is close to the caffeine peaks at  $613$  and  $644\text{ cm}^{-1}$ , and also overlaps with the shoulder of the strong caffeine peak at  $555\text{ cm}^{-1}$ . This has been a challenge in the identification of low-purity heroin samples in the past.<sup>[33]</sup>

SSRS provides two capabilities to help resolve weak Raman peaks in the presence of strong interference. First, the integration time can be increased near the peak(s) of

interest to improve the signal-to-noise ratio and sensitivity. Secondly, the spectrum could be sampled with a high resolution by reducing the step size during wavelength scanning. To keep the overall spectral acquisition time manageable, the laser could be swept over a more limited spectral range. This capability is demonstrated for the heroin sample in Figure 5b, in which the integration time per spectral point is increased to 5 s and the spectral step size is reduced to  $2\text{ cm}^{-1}$  — compared with 1 s and  $5\text{ cm}^{-1}$  used for the other spectra in the paper. Figure 5b shows the Raman spectra over 5 points on the sample acquired with the same acquisition settings. A few weak peaks are observed near  $620\text{ cm}^{-1}$ , close to the Raman peak of heroin.

In order to find a better understanding of the contribution of heroin to the acquired spectra from the sample, we utilized a two-step Bayesian estimation algorithm that our group has developed.<sup>[34]</sup> This algorithm is capable of finding the contribution of a target molecule to the Raman spectrum of a mixture with unknown chemicals and a strong background signal. In the first step, the algorithm decomposes the Raman spectrum of the target molecule on a series of modified Voigt functions that represent the Raman peaks of the spectrum. The algorithm uses a Reversible-jump Markov chain Monte Carlo (RJ-MCMC) technique to find the best fit of a series of modified Voigt functions to a Raman spectrum. In the second step, the same algorithm is used to decompose the Raman spectrum of the mixture on another series of modified Voigt functions. However, in this step, we include the contribution of the target molecule through its decomposed Raman peaks (Voigt functions found in the first step) with a single unknown weight that accounts for the concentration of the target molecule in the mixture. In the final step, the weight or concentration of the target molecule is one of the fitting parameters. At every fitting step, we also include a spline function to fit to the slowly varying fluorescence background.

We applied the algorithm to the Raman spectra of our sample and the target molecule, heroin hydrochloride (HCl) monohydrate. The fitting result to the Raman spectrum of the sample is shown by the dashed red curve in Figure 5c — the background is shown in green. Good agreement is observed between the measurement and the fitting result. The contribution of the Raman spectrum of heroin HCl monohydrate (black curve) along with all of the individual Raman peaks of unknown chemicals in the sample are shown in Figure 5d. Five of the major peaks in the decomposition belong to caffeine and are annotated in the figure. Even the weak Raman peak of caffeine at  $613\text{ cm}^{-1}$ , which is very close to the peak of heroin, was correctly found by the Bayesian algorithm.

As observed in Figure 5d, the Raman spectrum of heroin has a non-negligible contribution to the Raman spectrum of sample. However, to verify this is not a fitting error, we applied the same fitting algorithm to the Raman spectrum of pure caffeine as control. Because caffeine is the dominant cutting agent in our sample (all visible Raman peaks belong to caffeine) it can serve as a reasonable control in our experiment. We repeated the Bayesian fitting algorithm 40x on the Raman spectra of the sample and caffeine. The estimated heroin weight for is shown in Figure 5e. The difference between the contribution of heroin to the sample versus caffeine is about 5x larger than our fitting error. This control experiment provides confidence that the Bayesian algorithm is not confusing the Raman peaks of the cutting agent (caffeine) with those of the illicit substance.

## 4 | CONCLUSIONS

In summary, we demonstrated a swept-source Raman spectroscopy approach to address the sensitivity and background fluorescence limitations of the dispersive approach for the detection of low-purity illicit drugs. For the uncolored samples with low background fluorescence, we demonstrated that the swept-source approach provides a similar hit index to the target chemicals as with the dispersive system. We also demonstrated that longer excitation wavelengths into the 900 nm range is possible with the swept-source approach as compared with the dispersive approach due to the higher quantum efficiency available in low-cost infrared-enhanced silicon photodiodes. This allowed reducing the fluorescence emission by up to  $6\times$  in some of the colored drug samples. We also utilized the flexibility of the swept-source approach in adjusting the spectral resolution and integration time near the Raman peaks of interest to improve the spectral acquisition of weak Raman peaks. This allowed us to resolve the weak Raman peaks of a 1% heroin seized sample. To the best of our knowledge, this purity level is about 10x lower than the lowest heroin sample detected with spontaneous Raman spectroscopy. The results of our work demonstrate that the swept-source Raman spectroscopy approach is a promising solution for a host of samples with low concentration of the target molecule in the presence of a strong fluorescence background.

## ACKNOWLEDGEMENTS

This research was supported by the National Research Foundation (NRF), Prime Minister's Office, Singapore under its Campus for Research Excellence and Technological Enterprise (CREATE) program. The Disruptive & Sustainable Technology for Agricultural Precision

(DiSTAP) is an interdisciplinary research group (IRG) of the Singapore MIT Alliance for Research and Technology (SMART) Centre supported by the National Research Foundation (NRF), Prime Minister's Office, Singapore under its Campus for Research Excellence and Technological Enterprise (CREATE) program. K.X.E. K and T.W.L.S acknowledge the Central Narcotics Bureau (CNB), Singapore, for providing the seized illicit drugs analyzed in this work.

### CONFLICT OF INTERESTS

A.H.A is involved in developing Raman spectroscopy technologies at Perceptra Technologies. The rest of the authors have no conflict of interests to declare.

### ORCID

Amir H. Atabaki  <https://orcid.org/0000-0002-5020-5472>

### REFERENCES

- [1] United Nations Office on Drugs and Crime (UNODC), *World drug report 2020*, United Nations Publications **2020**.
- [2] National Institute on Drug Abuse (NIDA), Overdose death rates, Retrieved from: <https://www.drugabuse.gov/drug-topics/trends-statistics/overdose-death-rates>
- [3] M. Tan, T. Tan, Counting the cost: Drug abuse and drug crime in singapore, Retrieved from: <https://www.mha.gov.sg/hometeamnews/on-assignment/ViewArticle/counting-the-cost-drug-abuse-and-drug-crime-in-singapore>
- [4] Australian Criminal Intelligence Commission (ACIC), *Illicit drug data report 2015–16*. **2017**.
- [5] Australian Criminal Intelligence Commission (ACIC), *Illicit drug data report 2017–18*. **2019**.
- [6] Drug Enforcement Administration (DEA), Fentanyl signature profiling program report **2019**.
- [7] European Monitoring Centre for Drugs and Drug Addiction (EMCDDA), *Annual report 2012: The state of the drug problem in europe*, EMCDDA, Luxembourg **2012**.
- [8] European Monitoring Centre for Drugs and Drug Addiction (EMCDDA), *European drug report 2019: Trend and developments*, EMCDDA, Luxembourg **2019**.
- [9] United Nations Office on Drugs and Crime (UNODC), *Synthetic drugs in east and south-east asia trends and patterns of amphetamine-type stimulants and new psychoactive substances*, UNODC Global SMART Programme **2019**.
- [10] Drug Enforcement Administration (DEA), The 2016 heroin signature program report **2018**.
- [11] S. G. Mars, J. Ondocsin, D. Ciccarone, *J. Psychoact. Drugs* **2018**, 50(2), 167.
- [12] M. Sulaiman, V. Kunalan, ATW Yap, W. J. L. Lim, J. J. Y. Ng, S. W. X. Loh, K. B. Chan, *Drug Test. Anal.* **2018**, 10(1), 109.
- [13] C. W. Wright, S. D. Harvey, B. W. Wright, *Nondestruct Detect Meas Homeland Sec* **2003**, 5048, 107.
- [14] J. M. Lerner, A. Thevenon, *The optics of spectroscopy*, Instruments SA, Inc. **1988**.
- [15] C. A. F. de Oliveira Penido, L. Silveira Jr, M. T. T. Pacheco, *Instrum. Sci. Technol.* **2012**, 40(5), 441.
- [16] E. Gerace, F. Seganti, C. Luciano, T. Lombardo, D. Di Corcia, H. Teifel, M. Vincenti, A. Salomone, *Drug Alcohol Rev.* **2019**, 38(1), 50.
- [17] A. Guirguis, S. Giroto, B. Berti, J. L. Stair, *Forensic Sci. Int.* **2017**, 273, 113.
- [18] M. D. Hargreaves, A. D. Burnett, T. Munshi, J. E. Cunningham, E. H. Linfield, A. G. Davies, H. G. M. Edwards, *J. Raman Spectrosc.* **2009**, 40(12), 1974.
- [19] E. M. A. Ali, H. G. M. Edwards, R. Cox, *J. Raman Spectrosc.* **2015**, 46(3), 322.
- [20] A. Haddad, M. A. Comanescu, O. Green, T. A. Kubic, J. R. Lombardi, *Anal. Chem.* **2018**, 90(21), 12678.
- [21] A. H. Atabaki, W. F. Herrington, C. Burgner, V. Jayaraman, R. J. Ram, *Optics Express* **2021**, 29(16), 24723.
- [22] C. Cole, L. Jones, J. McVeigh, A. Kicman, Q. Syed, M. A. Bellis, *Cut: a guide to adulterants, bulking agents and other contaminants found in illicit drugs*, John Moores University, Liverpool **2010**.
- [23] Drug Enforcement Administration (DEA), *2019 national drug threat assessment*, DEA **2019**.
- [24] National Forensic Science Technology Center (NFSTC), *Evaluation of the thermo scientific® firstdefender raman spectrometer-technology evaluation*, National Institute of Justice **2010**.
- [25] A. G. Ryder, G. M. O'Connor, T. J. Glynn, *J. Forensic Sci.* **1999**, 44(5), 1013.
- [26] United Nations Office on Drugs and Crime (UNODC), *Global synthetic drugs assessment - amphetamine-type stimulants and new psychoactive substances*, United Nations Publications **2017**.
- [27] Office of National Drug Control Policy, *National drug control strategy data supplement 2020*. **2020**.
- [28] C. A. F. de Oliveira Penido, M. T. T. Pacheco, I. K. Lednev, L. Silveira Jr, *J. Raman Spectrosc.* **2016**, 47(1), 28.
- [29] Drug Enforcement Administration (DEA), Opium poppy cultivation and heroin processing in southeast asia **1992**.
- [30] R. McKetin, J. McLaren, *The methamphetamine situation in australia: A review of routine data sources*, National Drug Law Enforcement Research Fund **2004**.
- [31] L. S. A. Pereira, F. L. C. Lisboa, J. C. Neto, F. N. Valladão, M. M. Sena, *Forensic Sci. Int.* **2018**, 288, 227.
- [32] S. Lee, H. Lee, H. Chung, *Analytica chimica acta* **2013**, 758, 58.
- [33] A. G. Ryder, *J. Forensic Sci.* **2002**, 47(2), 275.
- [34] N. Han, R. J. Ram, *Comput. Stat. Data Anal.* **2020**, 143, 106846.

### SUPPORTING INFORMATION

Additional supporting information may be found in the online version of the article at the publisher's website.

**How to cite this article:** K. X. E. Kay, A. H. Atabaki, W. B. Ng, Z. Li, G. P. Singh, S. W. L. Tan, R. J. Ram, *J Raman Spectrosc* **2022**, 53(7), 1321. <https://doi.org/10.1002/jrs.6357>